LA-UR -83-2567

CONF-830942--36

Los Alamos National Laboratory is operated by the University of California for the United States Department of Energy under contract W-7405-ENG-36.

LA-UR--83-2567

DE84 001400

TITLE: IMPROVED ACTIVATION CROSS SECTIONS FOR VANADIUM AND TITANIUM

AUTHOR(S): D. W. Muir and E. D. Arthur

SUBMITTED TO: The Third Topical Meeting on Fusion Reactor Materials, Albuquerque, New Mexico, September 19-22, 1983

DISCLAIMER

MASTER

Los Alamos Los Alamos National Laboratory
Los Alamos, New Mexico 87545

IMPROVED ACTIVATION CROSS SECTIONS FOR VANADIUM AND TITANIUM

Douglas W. MUIR and Edward D. ARTHUR

Theoretical Division, Los Alamos National Laboratory, Los Alamos, New Mexico, U.S.A.

Vanadium alloys such as V-20Ti and V-Cr-Ti are attractive candidates for use as structural materials in fusion-reactor blankets. The virtual absence of long-lived activation products in these alloys suggest the possibility of reprocessing on an intermediate time scale. We have employed the modern Hauser-Feshbach nuclear-model code GNASH to calculate cross sections for neutron-activation reactions in ^{50}V and ^{51}V, to allow a more accurate assessment of induced radioactivity in vanadium alloys. In addition, cross sections are calculated for the reactions $^{46}Ti(n,2n)$ and $^{45}Ti(n,2n)$ in order to estimate the production of ^{44}Ti, a 1.2-MeV gamma-ray source with a half-life of 47 years.

1. INTRODUCTION

Vanadium alloys (such as V-20Ti and V-Cr-Ti) are attractive candidates for use as structural materials in fusion-reactor blankets both because of good mechanical properties at high temperatures and because of favorable activation characteristics.[1] The virtual absence[2] of long-lived neutron-activation products of vanadium, titanium, and chromium suggests the possibility of reprocessing and recycling vanadium-alloy blanket components after reasonably short cooling times (perhaps 30-50 years).

As discussed in Sections 3 and 4, we have used the nuclear-model code GNASH to calculate cross sections for several neutron-activation reactions in vanadium and titanium, in order to allow an accurate assessment of induced radioactivity in the time scale of interest for recycling, namely, 1 to 100 years. In addition, we have reviewed the available decay data for the radionuclides produced.

2. CALCULATIONS OF RADIOACTIVITY INDUCED IN V-20Ti

If one assumes that the noble-gas activation product ^{42}Ar ($t_{\frac{1}{2}}$ = 33 y) can be removed, for example by heating, and if one further assumes that the activation of impurities can be neglected, then the gamma-ray dose near an irradiated blanket component manufactured from V-20Ti will be dominated, in the first few years after removal from the reactor, by x-rays and internal bremsstrahlung photons from ^{49}V ($t_{\frac{1}{2}}$ = 0.90 y). After several years, most of the dose will come from hard gamma rays from ^{44}Ti ($t_{\frac{1}{2}}$ = 47 y). A summary of the decay properties of these two nuclides is given in Table I, along with the relevant 14.1-MeV production cross sections calculated with GNASH.

For radioactivity calculations, we have adopted an operating scenario in which a first wall of V-20Ti alloy is irradiated at a neutron wall loading of 10 MW/m^2 for a period, t, of two years (see Ref. 2). The neutron source is assumed to be uniformly distributed over a plasma region which extends from the center of a cylindrical vacuum vessel out to a plasma radius r_p, assumed to be equal to 0.7 times the first wall radius r_w. For this value of r_p/r_w, and independent of the actual wall radius, the flux of unscattered 14.1-MeV neutrons arriving at the first wall will be 1.69 times the 14.1-MeV neutron current, which at 10 MW/m^2 is 4.44 x 10^{14} n/cm^2 sec. The first-wall uncollided flux, ϕ, is then 7.50 x 10^{14} n/cm^2 sec. As shown in Section 4, all of the production reactions of interest here have high thresholds

and steeply rising excitation functions. Because of this, it is a reasonable approximation here to calculate radionuclide production rates from ϕ alone, ignoring the contribution from lower-energy scattered neutrons.

TABLE I.
Activation and Decay Data for V and Ti

	Cross Section at 14.1 MeV
$^{51}V(n,2n)$	0.524 b
$^{50}V(n,2n)$	0.692 b
$^{46}Ti(n,2n)$	0.0124 b
$^{45}Ti(n,2n)$	0.0926 b

	Half Life	Photon Energy	Photons Per Decay
^{49}V	0.90 y	~ 300 keV[a]	~ 0.0003[b]
		4.5 keV[c]	0.196
^{44}Ti	47 y	2.656 MeV	0.001
		1.499 MeV	0.009
		1.157 MeV	0.999

[a] Internal bremsstrahlung accompanying electron capture. The spectrum is a broad continuum extending from 0 up to 616 keV. (See Ref. 3.)

[b] Absolute intensity estimated from Eq. (8) of Ref. 4.

[c] Private communications from J. K. Tuli and D. C. Kocher.

In this approximation, at the end of the irradiation, the ratio of ^{49}V to initial total vanadium atoms will be

$$\frac{n_{49}}{n_V} = 0.9975 \times (\sigma_{51}\,\phi\,t) \times (\sigma_{50}\,\phi\,\tfrac{t}{2}) \times 0.636 + 0.0025 \times (\sigma_{50}\,\phi\,t) \times 0.510 \quad ,$$

where the first contribution results from the two-step process ($^{51}V \rightarrow ^{50}V \rightarrow ^{49}V$), while the second results from direct production from the 0.25% abundant ^{50}V in natural vanadium. The fractions 0.636 and 0.510 are the respective probabilities that a ^{49}V atom born during the reactor irradiation will survive until the end of irradiation in these two production modes. Inserting numerical values from Table I, we obtain

$$\frac{n_{49}}{n_V} = 3.02 \times 10^{-4} \quad , \qquad (1)$$

with about 86% of the ^{49}V atoms resulting from the two-step process.

Similarly, the ratio of ^{44}Ti atoms to initial total titanium atoms is calculated as

$$\frac{n_{44}}{n_{Ti}} = 0.082 \times (\sigma_{46}\,\phi\,t) \times (\sigma_{45}\,\phi\,\tau_{45}) \quad ,$$

where τ_{45}, the average lifetime of a ^{45}Ti atom, is 1.60×10^4 s. Again inserting numerical values, we obtain

$$\frac{n_{44}}{n_{Ti}} = 5.37 \times 10^{-11} \quad . \qquad (2)$$

In spite of the very low gamma-ray intensity from ^{49}V decays, it is clear from the results in Eqs. (1) and (2) that, at early times, ^{49}V will dominate ^{44}Ti as a source of energetic gamma rays. It is also clear that, after about ten years of storage, ^{44}Ti will dominate.

It is of interest to evaluate the gamma-ray dose rate at the surface of a large, thick sheet of V-20Ti alloy. A useful formula for this is given in Ref. 2,

$$\text{Dose (R/h)} = 6.57 \times 10^{-5} \sum_{\text{all } \gamma \text{ lines}} \bar{\mu}_a\, S_\gamma\, \frac{B}{2\mu_m} \quad , \qquad (3)$$

where $\bar{\mu}_a$ is the energy absorption coefficient of air ($cm^2\ g^{-1}$), μ_m is the linear attenuation

coefficient of the alloy ($cm^2\ g^{-1}$), S_γ is the rate of gamma-ray energy emission per unit mass (MeV $g^{-1}\ s^{-1}$), and B is the gamma-ray dose build-up factor, a number around 2. At late times, this result will be dominated by the 1.16-MeV gamma-ray from ^{44}Ti. Substituting the appropriate values in Eq. (3), we obtain the late-time dose rate,

$$\text{Dose} = 2^{-t/47} \times 2.25\ \text{mR/hour} \quad ,$$

where t is measured in years.

This level of radiation is about equal to the limit set by the U.S. government for radiation workers (1250 mrem in any 3-month period). While certainly not negligible, it probably would not present a serious obstacle to performing industrial operations, such as fabrication, with recycled V-20Ti. Of course, a definitive statement regarding the feasibility of recycling cannot be made here, since we have not included the dose from the activation of impurities.

3. CROSS-SECTION CALCULATIONAL METHODS

In order to obtain the activation cross sections used in this study, we employed the GNASH[5] multistep Hauser-Feshbach nuclear model code. This code handles complicated reaction chains and incorporates physics features, such as preequilibrium emission, necessary to adequately describe 14-MeV neutron interactions with nuclei. However, to utilize such a code effectively, input parameters must be determined using a wide variety of data sources, not just those directly related to the calculational problem of interest. For example, the theoretical description of neutron emission requires knowledge of neutron transmission coefficients over an extended energy range (~0.1-20.0 MeV). These we calculate using optical model parameters obtained by simultaneous fits to resonance data (s- and p-wave strengths, scattering radii[6]), as well as total and elastic cross sections. We followed such a procedure to fit data pertinent to the titanium and vanadium isotopes of interest here and the resulting neutron optical parameters appear in Table II.

We likewise followed a similar procedure for charged particle transmission coefficients. We began with global parameter sets[7,8] and adjusted them to optimize agreement with experimental data, principally elastic-scattering angular distributions and nonelastic cross sections. The resulting parameters were further validated through (p,n) and (α,n) cross-section calculations for nearby nuclei. Since several of the nuclei of interest to this study exhibit significant amounts of neutron-induced charged-particle emission, the proper behavior of these transmission coefficients is essential to the correct theoretical description of such processes, particularly (n,np) reactions.

Independent data were likewise used in the determination of the remaining input parameters, in particular, the gamma-ray strength function and the nuclear level density. For the strength function, we assumed a giant-dipole resonance shape[9] and normalized it to reproduce (n,γ) cross sections for several nuclei in this mass region. The form of the nuclear level density was taken to be that given by the Gilbert-Cameron model.[10] This model was utilized in conjunction with the maximum amount of discrete nuclear level information[11] available for each residual nucleus occurring in the reaction sequence. To determine the pertinent model parameters, we simultaneously fitted data for the cumulative number of levels occurring at a given excitation energy as well as available s-wave resonance-spacing information.[6]

TABLE II

Neutron Optical Parameters Obtained for Titanium and Vanadium Isotopes*

		r	a
Ti	$V = 49.46 - 0.192E$	1.261	0.6
	$W_{VOL} = -0.544 + 0.39E$	1.261	0.6
	$V_{SO} = 6.2$	1.12	0.47
	$W_{SD} = 3.975 + 0.074E$	1.364	0.42
	for E_n>6 MeV		
	$W_{SD} = 4.419 - 0.1(E-6)$	1.364	0.42
V	$V = 48.86 - 0.43E + 0.0003E^2$	1.292	0.6076
	$W_{VOL} = -0.207 + 0.253E$	1.292	0.6076
	$V_{SO} = 6.2$	1.12	0.47
	$W_{SD} = 4.91 + 0.074E$	1.3685	0.429
	for E_n>6 MeV		
	$W_{SD} = 5.354 - 0.17(E-6)$	1.3685	0.429

*All well depths in MeV; geometrical parameters in fermis.

As a final preparatory step in our calculational effort, we computed direct-reaction contributions to neutron inelastic scattering cross sections from collective levels using the Distorted Wave Born Approximation (DWBA). Such contributions are important over the energy range of interest and cannot be described using Hauser-Feshbach or preequilibrium models. To determine the deformation parameters necessary for normalization of the DWBA results, we used values[12,13] obtained from proton inelastic scattering measurements.

4. CROSS-SECTION RESULTS

With these preparations complete, we proceeded to cross-section calculations on ^{45,46}Ti and ^{50,51}V, some results of which appear in Fig. 1. Calculated ^{46}Ti(n,2n) cross sections (solid curve) are compared to data[14] in the energy range from threshold to 16 MeV. The agreement is good, especially considering that no attempt has been made to optimize the calculations to this particular reaction. Within this energy range the theoretical cross section for the (n,2n) reaction involves only population of discrete levels in ^{45}Ti so that the proper energy behavior of neutron transmission coefficients is essential for realistic results. Equally important is the proper description of competing reactions, particularly those involving charged-particle emission, since they dominate for this target nucleus. The calculations simultaneously reproduce such data well, as illustrated in Fig. 2 where a comparison is made to the ^{46}Ti proton spectrum[15] induced by 15-MeV neutrons. The agreement is particularly significant in the low-energy portion of the spectrum, since this region encompasses protons

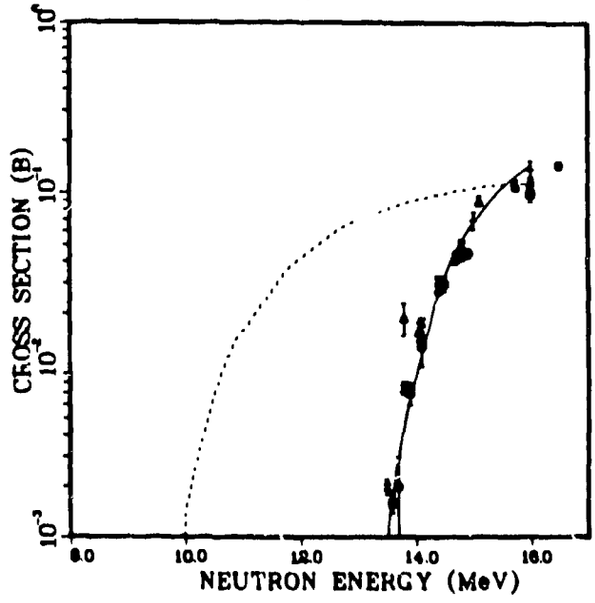

FIGURE 1.

Calculated ^{45,46}Ti(n,2n) values are compared to experimental data.[14] The dashed curve represents ^{45}Ti results while the solid curve indicates similar cross sections for ^{46}Ti(n,2n).

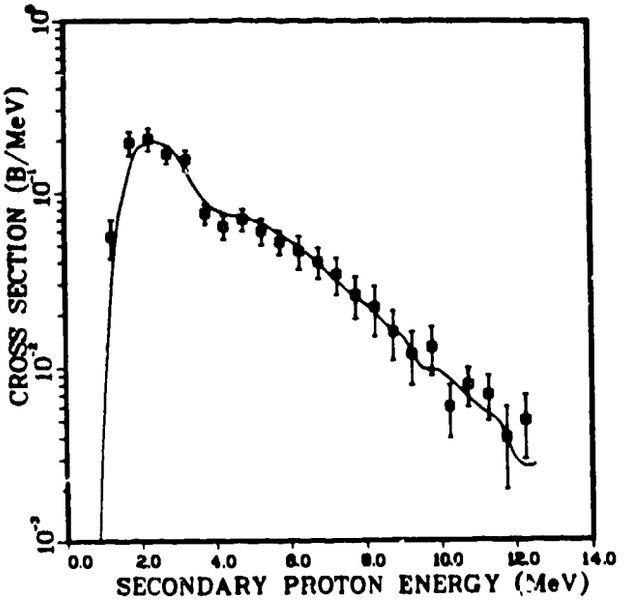

FIGURE 2.
The calculated proton emission spectrum induced by 15-MeV neutrons on ^{46}Ti is compared to experimental data.[15]

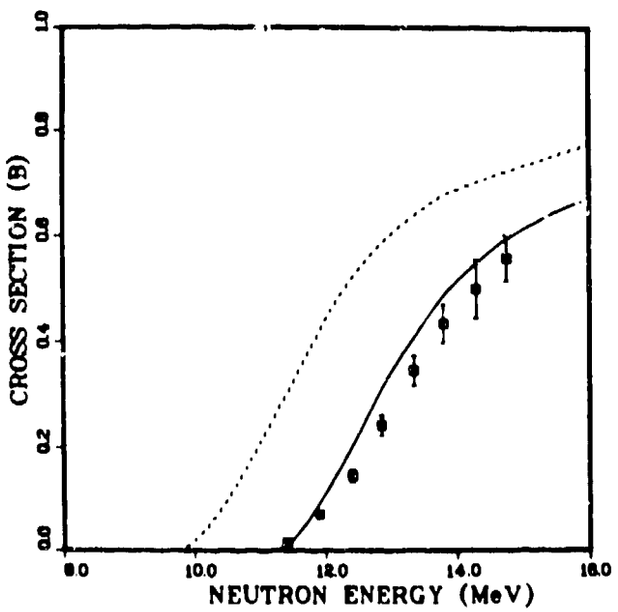

FIGURE 3.
Calculated ^{51}V(n,2n) (solid curve) and ^{50}V(n,2n) (dashed curve) cross sections are compared to available experimental results[14] (for ^{nat}V).

from the (n,np) process that compete directly with the (n,2n) reaction. Returning to Fig. 1, the dashed curve shows the predicted behavior of the (n,2n) reaction on the unstable ($t_{1/2}$ = 3.08 h) ^{45}Ti target nucleus. Although the ^{45}Ti (n,2n) threshold lies significantly lower than for ^{46}Ti(n,2n), the 14-MeV cross section is still fairly small (less than 100 mb), because of sizable competition from charged-particle emission.

Figure 3 compares calculated (n,2n) cross sections with data[14] available for naturally-occurring vanadium isotopes. In this instance, neutron emission is the dominant reaction mechanism rather than charged-particle emission as was the case previously for ^{45,46}Ti. [We did, however, compare our calculations with measured values of ^{51}V(n,p) and (n,α) reactions where we found agreement on the order of 10%, even though cross-section magnitudes were small compared with (n,2n) values.] For such (n,2n) reactions the calculations are dominated by transitions to discrete levels in the ^{49,50}V residual nuclei, so again a realistic low-energy description of the neutron transmission coefficients is important. The dashed curve illustrates the calculated ^{50}V(n,2n) cross section for which no experimental data exists. Its threshold lies about 2 MeV lower than for ^{51}V(n,2n), but around 14-MeV the cross sections are comparable.

5. CONCLUSIONS

These examples illustrate the use of a modern nuclear reaction code such as GNASH to calculate activation cross sections important for fusion reactor applications. These results also illustrate that, with proper care in parameter determination, realistic theoretical cross sections can be obtained even in the case of minor reaction paths. Such calculations can thereby be used with confidence to provide nuclear data in instances where experimental

measurements are difficult (such as on a rare isotope) or totally impractical, as in cases involving unstable targets.

REFERENCES

1. D. Steiner, Nuclear Fusion 14, 33(1974)

2. O. N. Jarvis, "Selection of Low-Activity Elements for Inclusion in Structural Materials for Fusion Reactors," UKAEA Harwell report AERE-R 10496 (1982).

3. R. W. Hayward and D. D. Hoppes, Phys. Rev. 104, 183 (1956).

4. B. G. Pettersson, "Internal Bremsstrahlung," Chap. XXV (D) of "Alpha-, Beta-, and Gamma-Ray Spectroscopy, Vol. 2," K. Siegbahn, Ed., North-Holland Publishing Company, Amsterdam (1965).

5. P. G. Young and E. D. Arthur, "GNASH: A Preequilibrium Statistical Nuclear Model Code for Calculation of Cross Sections and Emission Spectra," Los Alamos National Laboratory report LA-6947 (1977).

6. S. F. Mughabghab, M. Divadeenam, and N. E. Holden, Neutron Cross Sections Vol. 1 (Academic Press, New York, 1981).

7. F. G. Perey, Phys. Rev. 131 (1962) 745.

8. O. F. Lemos, "Diffusion Elastique de Particules Alpha," Orsay report A136 (1972).

9. P. Axel, Phys. Rev. 126 (1962) 671.

10. A. Gilbert and A. G. W. Cameron, Can. J. Phys. 43 (1965) 1446.

11. C. Michael Lederer and Virginia S. Shirley, Table of Isotopes, Seventh Edition (John Wiley & Sons, Inc., New York, 1978).

12. R. J. Peterson, Ann. of Physics 53 (1969) 40.

13. H. F. Lutz et al., Phys. Rev. 187 (1969) 1479.

14. Experimental data provided from the CSISRS compilation by the National Nuclear Data Center, Brookhaven National Laboratory, Upton, N.Y.

15. S. Grimes et al., Nucl. Sci. Eng. 6_ (1977) 187.